doi:10.1093/scan/nsu005 SCAN (2014) 9, 2017–2025

Functional connectivity with ventromedial prefrontal cortex reflects subjective value for social rewards

David V. Smith,[1,2] John A. Clithero,[3] Sarah E. Boltuck,[1] and Scott A. Huettel[1,2,*]
[1]Center for Cognitive Neuroscience, [2]Department of Psychology and Neuroscience, Duke University, Durham, NC 27708, and [3]Division of the Humanities and Social Sciences, California Institute of Technology, Pasadena, CA 91125, USA

According to many studies, the ventromedial prefrontal cortex (VMPFC) encodes the subjective value of disparate rewards on a common scale. Yet, a host of other reward factors—likely represented outside of VMPFC—must be integrated to construct such signals for valuation. Using functional magnetic resonance imaging (fMRI), we tested whether the interactions between posterior VMPFC and functionally connected brain regions predict subjective value. During fMRI scanning, participants rated the attractiveness of unfamiliar faces. We found that activation in dorsal anterior cingulate cortex, anterior VMPFC and caudate increased with higher attractiveness ratings. Using data from a post-scan task in which participants spent money to view attractive faces, we quantified each individual's subjective value for attractiveness. We found that connectivity between posterior VMPFC and regions frequently modulated by social information—including the temporal-parietal junction (TPJ) and middle temporal gyrus—was correlated with individual differences in subjective value. Crucially, these additional regions explained unique variation in subjective value beyond that extracted from value regions alone. These findings indicate not only that posterior VMPFC interacts with additional brain regions during valuation, but also that these additional regions carry information employed to construct the subjective value for social reward.

Keywords: valuation; faces; connectivity; social reward; VMPFC

INTRODUCTION

Difficult choices rarely involve simple comparisons along a single attribute. More commonly, a decision requires comparing disparate goods with incommensurable attributes and properties. Understanding the neural mechanisms that construct common values has been a cardinal goal of decision neuroscience (Smith and Huettel, 2010; Padoa-Schioppa, 2011; Rushworth *et al.*, 2011; Wallis, 2012). Several studies have converged on the observation that ventromedial prefrontal cortex (VMPFC) (Chib *et al.*, 2009; FitzGerald *et al.*, 2009; Kim *et al.*, 2011; Lin *et al.*, 2012) and striatum (Izuma *et al.*, 2008; Clithero *et al.*, 2011a) contain spatially overlapping subjective value signals for multiple goods (e.g. money, food, social images and consumer goods) (meta-analytic data reviewed in Clithero and Rangel, 2013). Extending these findings, other work has indicated that a posterior region within VMPFC (pVMPFC) encodes different rewards on a common scale in which idiosyncratic behavioral values are matched to neural values within pVMPFC (Smith *et al.*, 2010; Levy and Glimcher, 2011; Zaki *et al.*, 2013), even across different states (Libedinsky *et al.*, 2011), suggesting pVMPFC activation encodes a common neural currency (for review, Levy and Glimcher, 2012).

Far less is known, however, about how common currency and subjective value signals in pVMPFC are modulated by information represented in other brain systems. At the most basic level, punishment and reinforcement information, whose neural correlates are distributed throughout the brain (Vickery *et al.*, 2011), should be expected to contribute to the construction of subjective value. In many cases, these computations must also incorporate diverse contextual cues about our social environment, which influence our interpersonal interactions and guide social decision making (Fehr and Camerer, 2007). Central to many social decisions is the need to evaluate the intentions of others, a process that evokes activation across a network of regions, including the temporal-parietal junction (TPJ), medial prefrontal cortex (MPFC), and posterior cingulate cortex (PCC) (Saxe, 2006; Behrens *et al.*, 2009; Hasson *et al.*, 2012). Although studies employing functional connectivity analyses have made progress in identifying regions that interact with pVMPFC during decision making (Hare et al., 2009, 2010; Park *et al.*, 2011), it remains unclear how additional regions contribute to our idiosyncratic social valuations.

We hypothesized that social valuation depends on interactions between pVMPFC and regions modulated by social information in our task, particularly the TPJ, which appears to make a unique contribution to the establishment of a social context for decision making (Carter *et al.*, 2012). Unlike prior work investigating functional connectivity between pVMPFC and TPJ (Hare, *et al.*, 2010; van den Bos *et al.*, 2013), we also examined how the strength of connectivity with pVMPFC predicts individual differences in subjective value for social stimuli and whether functionally connected regions such as TPJ predict unique variation in trial-to-trial assessments of value. To test these hypotheses, we used a task in which participants rated attractive faces on each trial (Figure 1A). Following the fMRI session, participants engaged in an economic exchange task (Smith *et al.*, 2010) that allowed us to assess each participant's subjective value for those social images (Figure 1B). We employed a functional connectivity analysis to determine which regions increase connectivity with pVMPFC during social valuation. Crucially, we also used a hierarchical regression analysis to evaluate whether activation in these functionally connected pVMPFC regions explains additional variation in social valuation over and beyond activation from regions modulated by value. Our results indicated that connectivity between pVMPFC and a network of regions—including TPJ, PCC and MPFC—predicted individual differences in social valuation, supporting the idea that these regions contribute to computation of subjective value for social reward.

Received 23 April 2013; Revised 4 December 2013; Accepted 10 January 2014
Advance Access publication 3 February 2014

*Present address: Department of Psychology, Rutgers University, Newark, NJ 07102, USA.

We thank Dominic Fareri and Jacob Young for helpful comments on previous drafts. This work was supported by the National Institute of Mental Health [National Research Service Award F31-086248 to D.V.S.]; the Duke Institute for Brain Sciences [Incubator Award to S.A.H.].

Correspondence should be addressed to Scott A. Huettel, Ph.D, Department of Psychology and Neuroscience, Duke University, Box 90999, Durham, NC 27708 USA. E-mail: scott.huettel@duke.edu

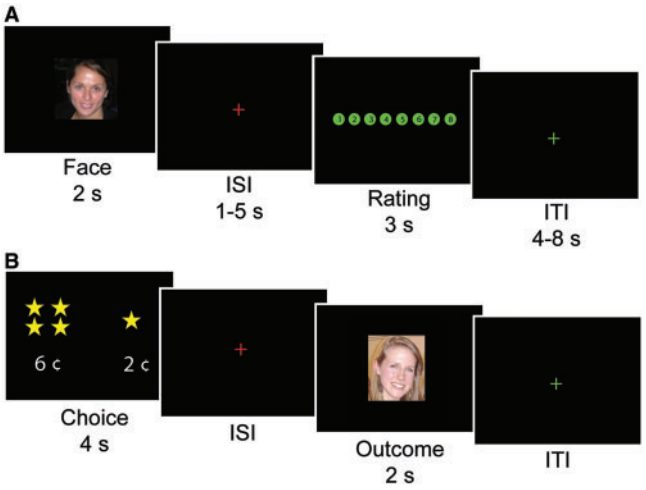

Fig. 1 Experimental tasks. (**A**) Trial structure for the ratings task. Male, heterosexual young adults viewed a randomized sequence of images of female faces and provided, for each image, an attractiveness rating using an 8-point scale. To control for motor anticipation, the ordering of the 8-point scale was randomly flipped across trials; on half of the trials, the highest rating was the left-most option and on the other half of the trials, the highest rating was the right-most option (as shown in the example). (**B**) Trial structure for the economic exchange task. Each trial began with a choice phase (lasting 4 s) in which the participant was forced to spend a small amount of money to view a face. Participants could choose to spend more money to view a more attractive face (denoted with increasing stars) or less money to view a less attractive face. After a variable delay period, a single face, randomly selected from the chosen attractiveness category, was displayed for 2 s.

MATERIALS AND METHODS

Participants

In total, 20 self-reported heterosexual males with normal or corrected-to-normal vision completed the study (mean age: 23 years, range: 18–30 years). We excluded four of these individuals prior to data analyses (three for head movement >2 mm and one because of equipment failure), leaving a final sample of 16 participants. Pre-screening excluded individuals with prior psychiatric or neurological illness. All participants provided written informed consent as part of a protocol approved by the Institutional Review Board of Duke University Medical Center.

Stimuli and tasks

In the scanner, participants engaged in two 36-trial runs of a social reward evaluation task (Figure 1A). Social rewards were images of female faces, drawn equally from two attractiveness categories (medium–high and medium–low) determined by a previous study (Smith *et al.*, 2010). (Due to technical error, three participants only received images from the medium–high category; however, these three participants were indistinguishable from the other 13 participants on all behavioral measures.) On each trial, a single social reward image was shown for 2 s and then followed by a variable fixation period (1–5 s). After the fixation period, an 8-point rating scale was shown for 3 s, while participants expressed their attractiveness rating using a magnetic resonance imaging (MRI)-compatible button box; after the response, the color of the selected rating changed to red. Although trial-to-trial attractiveness ratings allow us to examine parametric changes along a specific social dimension, we note that attractiveness itself could be driven by unmeasured factors associated with either social or non-social properties of the faces (O'Doherty *et al.*, 2003). Nevertheless, that faces have idiosyncratic value across subjects makes them an ideal good for studying value computations. To control for motor anticipation, the scale ordering was randomly counterbalanced (left–right or right–left) from trial to trial. Trials were separated by a variable intertrial interval (ITI) of 4–8 s. The scanner session also contained another, passive viewing task (results reported elsewhere: Clithero *et al.*, 2011b). Stimuli were projected onto a screen at the back of the scanner bore and participants viewed the stimuli through mirrored goggles.

Following the scanner session, participants performed an economic exchange task (Figure 1B) (Smith *et al.*, 2010; Clithero *et al.*, 2011b). On each trial, participants chose whether to spend more money to view a novel high attractiveness face or less money to view a novel low attractiveness face. Monetary cost ranged from 1 to 12 cents, whereas attractiveness spanned four distinct categories (1–4 stars for increasing attractiveness). Both cost and attractiveness varied randomly across trials within uniform distributions, with the constraints that the two face options always differed in attractiveness and that the more attractive face always carried the greater monetary cost. After a 4 s decision window, the screen went blank for a variable fixation interval of 2–4 s before a face from the chosen category was presented for 2 s. Participants made 48 decisions during the economic exchange task.

Tasks were programed using the Psychophysics Toolbox version 2.54 (Brainard, 1997) for MATLAB. Cash payment was determined by adding the cumulative total of a randomly selected run from the passive viewing task (Clithero *et al.*, 2011b) to a base payment of $50 and then subtracting the total amount spent during the economic exchange task. Participants received an average of $16 for their bonus reward and spent an average of $2.12 to view new faces in the economic exchange task, resulting in a total mean payment of ~$66 (range $53–92). Participants were provided full information regarding the payment mechanism prior to the scanning session.

Prior to analyses, we normalized each participant's attractiveness ratings by converting the raw ratings from 1 to 8 scale into a 0 to 1 scale (minimum to maximum). We then grouped the normalized ratings by quintiles, representing the lowest quintile with a 1 and the highest quintile with a 5. This normalization procedure controls for individual response bias and facilitates comparison across participants. Aside from one participant who only used four numbers in his ratings, all participants could be mapped to the normalized 1–5 scale. This participant, though indistinguishable from the remainder of our sample on all behavioral measures, could not be included in the medium attractiveness category as shown in Figure 2B. Nevertheless, we emphasize that our core inferences are based on analysis of the parametric effects of increasing attractiveness judgments, which allows this participant to be included in the same model as the other participants.

Image acquisition

Neuroimaging data were acquired on a 3-Tesla General Electric scanner with an 8-channel parallel imaging system. Images sensitive to blood oxygenation level-dependent (BOLD) contrast were acquired using a T_2*-weighted gradient-echo echo-planar imaging (EPI) sequence, with slices parallel to the axial plane connecting the anterior and posterior commissures [repetition time (TR): 2000 ms; echo time (TE): 27 ms; matrix: 64 × 64; field of view (FOV): 240 mm; voxel size: 3.75 × 3.75 × 3.8 mm; 34 axial slices; flip angle: 60°]. Prior to analysis, the first seven volumes of each run were discarded to allow for magnetic stabilization. We also acquired whole-brain high-resolution anatomical scans to aide in normalization and co-registration (T_1-weighted FSPGR sequence; TR: 7.3 ms; TE: 2.9 ms; matrix: 256 × 256; FOV: 256 mm; voxel size: 0.93 × 0.93 × 1.9 mm; 68 axial slices; flip angle: 12°).

FMRI pre-processing

For pre-processing, we used tools from the FMRIB Software Library (FSL Version 4.1.5; http://www.fmrib.ox.ac.uk/fsl/) package (Smith *et al.*, 2004; Woolrich *et al.*, 2009). We first corrected for head

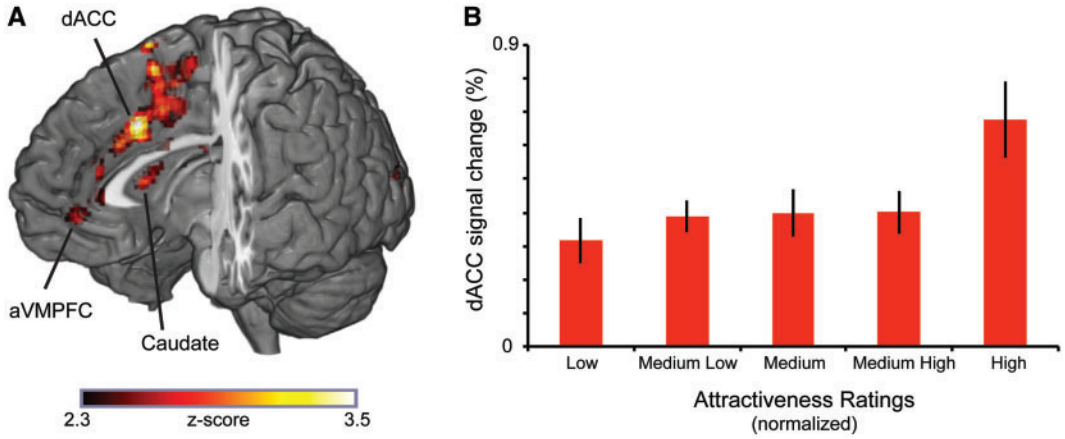

Fig. 2 Brain regions tracking increasing attractiveness judgments. (**A**) To identify brain regions whose activation tracked attractiveness judgments, we constructed parametric model based on each participant's ratings. Brain regions tracking attractiveness ratings included the dorsal anterior cingulate cortex (dACC) (x,y,z = 6,18,34), right caudate (x,y,z = 8,12,8), parts of visual cortex (x,y,z = −4,−100,4; x,y,z = −28,−82,2) and aVMPFC (x,y,z = 0,46,−8) (Table 1). All areas of activation passed an initial cluster-forming threshold of $z = 2.3$, with whole-brain cluster correction at $P = 0.05$ (corrected for multiple comparisons). (**B**) Interrogation of the dACC region revealed a quasi-linear trend of activation, with higher activation corresponding to higher ratings and lower activation corresponding to lower ratings. Error bars reflect SEM.

motion by realigning the time series to the middle volume (Jenkinson *et al.*, 2002). Non-brain material was then removed using the brain extraction tool (Smith, 2002). We corrected for intravolume slice-timing differences using Fourier-space phase shifting, aligning to the middle slice. Spatial smoothing employed a Gaussian isotropic kernel of full-width half-maximum 6 mm. The entire 4D dataset was grand mean intensity normalized using a single multiplicative factor. To remove low frequency drift in the MR signal, we used a high-pass temporal filter with a 100 s cutoff (Gaussian-weighted least-squares straight line fitting, with $\sigma = 50$ s). Functional data were spatially normalized to the Montreal Neurological Institute (MNI) avg152 T_1-weighted template (2 mm isotropic resolution) using a 12-parameter affine transformation implemented in FMRIB's Linear Image Registration Tool (FLIRT) (Jenkinson and Smith, 2001); these transformations were later applied to the statistical images before cross-run and cross-participant analyses.

As part of our pre-processing, we also identified outlier volumes in our functional data. We identified outlier volumes in our functional data by examining the root-mean-square error (RMSE) of each volume relative to a reference volume (the middle time point). A volume was considered an outlier if its RMSE amplitude exceeded the 75th percentile plus the value of 150% of the interquartile range of RMSE for all volumes in a run (i.e. a standard boxplot threshold). We excluded runs in which more than 12% of the time series was corrupted by outliers; this threshold corresponded to the 95th percentile of a distribution containing the proportion of outlier volumes across all runs of data in our sample. As a result of this threshold, one run was removed from five participants. These participants were otherwise indistinguishable from other participants with two runs of data.

FMRI analyses

Neuroimaging analyses were conducted using FEAT (FMRI Expert Analysis Tool) Version 5.98 (Smith *et al.*, 2004; Woolrich *et al.*, 2009). We employed two distinct models corresponding to our core hypotheses. Our first 'parametric' model examined brain regions whose activation increases as a function of increasing attractiveness ratings. Our first-level analysis (i.e. within run) used a general linear model (GLM) with local autocorrelation correction (Woolrich *et al.*, 2001). Each first-level GLM consisted of four regressors modeling the presentation of the face stimulus (duration = 2 s) and the ratings screen that followed the face (duration = 3 s). The regressor for the face stimulus was parametrically modulated by a series of polynomial expansions (first and second order) of the normalized participant-specific attractiveness ratings for each trial (Buchel *et al.*, 1998). The quadratic term (i.e. the second-order expansion) increases confidence in attributing response profiles; that is, if only a first-order term was used, underlying quadratic relationships could be misinterpreted as linear (Buchel *et al.*, 1998; Winston *et al.*, 2007; Mende-Siedlecki *et al.*, 2013). We examined the response profile in regions showing parametric effects by estimating an independent categorical model where response levels were modeled separately.

Our second 'psychophysiological interaction' (PPI) model (Friston *et al.*, 1997) identified voxels whose functional connectivity with pVMPFC increased as a function of increasing attractiveness ratings at the time of viewing the face. This region was chosen because of its role in value-based decision making (for review, Rangel and Hare, 2010; Smith and Huettel, 2010; Levy and Glimcher, 2012). We note that our previous work indicates that distinct subregions of VMPFC encode different aspects of value, where anterior VMPFC (aVMPFC) represents experienced value for multiple goods, whereas pVMPFC represents the relative decision value between multiple goods in the absence of choice (Smith *et al.*, 2010). Similar anatomical dissociations within VMPFC have been reported in recent meta-analytic work (Clithero and Rangel, 2013) and concurrent brain stimulation and fMRI work (Baumgartner *et al.*, 2011), although susceptibility-related distortions and different imaging parameters limit the specificity of anatomical comparisons across studies (Roy *et al.*, 2012). Our PPI model utilized the same regressors as the parametric model, but also included each participant's average time course within a 5-mm radius region of interest (ROI) in pVMPFC (MNI: x,y,z = 6,26,−14) reported in our previous work (Smith *et al.*, 2010). Using this a priori ROI from our previous work is important, as our imaging paradigm only presents one reward modality, which may limit our observed activation for attractiveness to aVMPFC (i.e. experienced value). Thus, examining signals related to decision value (which should be related to subsequent exchanges between faces and money), we use the pVMPFC ROI from our previous work. To form the PPI regressor, we multiplied the physiological regressor derived from pVMPFC by the regressor modeling the normalized participant-specific attractiveness ratings for each face presentation (i.e. the first-order parametric term from our first model). Although the collinearity between these regressors reduces power, including task variables and physiological signals

ensures that any observed PPI effects are specific to task-dependent changes in functional connectivity, rather than only changes in functional connectivity or only changes in task activation (O'Reilly *et al.*, 2012). We also note that directionality cannot be inferred from PPI effects and thus our claims are limited to interactions between pVMPFC and functionally connected brain regions (i.e. we cannot test whether these other regions are providing direct inputs into pVMPFC).

In both models, we included nuisance regressors to account for response time differences across ratings, missed ratings and outlier volumes due to head motion (Power *et al.*, 2012; Satterthwaite *et al.*, 2012). Except for the outlier volume nuisance regressors (which were unconvolved), all regressors were convolved with a canonical hemodynamic response function. We combined data across runs, for each subject, using a fixed-effects model and combined data across subjects using a mixed-effects model (Beckmann *et al.*, 2003; Woolrich *et al.*, 2004).

All z-statistic (Gaussianized t) images were thresholded using an initial cluster-forming threshold of $z > 2.3$ followed by a corrected cluster significance threshold of $P < 0.05$ (Worsley, 2001). All activation clusters survived additional correction for outliers (Woolrich, 2008). Statistical overlay images were created using MRIcron and MRIcroGL (Rorden *et al.*, 2007). As Brodmann labels do not depict anatomical variation (Zilles and Amunts, 2010), we show probabilistic anatomical labels for local activation maxima using the Harvard–Oxford cortical and subcortical atlases (Desikan *et al.*, 2006). All coordinates are reported in MNI space.

Trial-to-trial analysis

We constructed a trial-by-trial model that considered each face presentation separately—thus capturing trial-specific processes and interactions (cf. Rissman *et al.*, 2004). We extracted, for each trial, the median percent signal change within key ROIs identified from the parametric and PPI models described above. For each ROI, we first normalized the median parameter estimates by converting to z-scores and then excluded outliers (i.e. trials falling outside of the 2.5th or 97.5th percentiles). The resulting values were then used as factors in a hierarchical regression analysis performed in Stata 12.1 (StataCorp) using the *nestreg* function.

Our hierarchical regression evaluated the contribution of four distinct blocks of factors that predicted image ratings across all 711 trials (pooled across participants). The first block of factors controlled for potential confounds, including response time, trial number, run number and participant identity. This matrix of confound regressors is represented with *X_CON* in equation (1), where i indexes the trial number:

$$\text{Rating}_i = \beta_0 + X\_CON_i\beta_{\text{Block1}} + \varepsilon_i \quad (1)$$

Next, we added a second block of factors that included activation estimates within regions whose activation increased with higher attractiveness ratings. We also included activation estimates from pVMPFC and aVMPFC (MNI: x,y,z = 0,46,−8) derived in our previous work (Smith *et al.*, 2010). Individual differences in exchange rates (i.e. willingness to purchase faces in the economic exchange task) were modeled by including scaled versions of each regressor. We computed these scaled regressors by transforming the exchange rates to a −1 to 1 scale, demeaning and then multiplying the demeaned activation estimates, for each participant, by the transformed participant-specific exchange rate. Crucially, including participant-specific exchange rates in all blocks of factors allows our regression model to isolate effects that explain unique variance in trial-to-trial ratings over and above exchange rates alone. The complete matrix of value regressors is denoted with *X_VAL* in equation (2), where i indexes the trial number:

$$\text{Rating}_i = \beta_0 + X\_CON_i\beta_{\text{Block1}} + X\_VAL_i\beta_{\text{Block2}} + \varepsilon_i \quad (2)$$

Our third block of factors included activation estimates from regions exhibiting a PPI effect using pVMPFC as a seed. Individual differences in exchange rates in each of these regressors were modeled using the same procedure described for equation (2). This matrix of connectivity regressors is denoted with *X_PPI* in equation (3), where i indexes the trial number:

$$\text{Rating}_i = \beta_0 + X\_CON_i\beta_{\text{Block1}} + X\_VAL_i\beta_{\text{Block2}} + X\_PPI_i\beta_{\text{Block3}} + \varepsilon_i \quad (3)$$

Our fourth block of factors—corresponding to the full regression model—included terms that modeled the interaction between pVMPFC and the regions exhibiting a PPI effect. As before, we modeled individual differences in exchange rates in each of these regressors using the same procedure described for equation (2). This matrix of interaction regressors is denoted with *X_INT* in equation (4), where i indexes the trial number:

$$\text{Rating}_i = \beta_0 + X\_CON_i\beta_{\text{Block1}} + X\_VAL_i\beta_{\text{Block2}} + X\_PPI_i\beta_{\text{Block3}} + X\_INT_i\beta_{\text{Block4}} + \varepsilon_i \quad (4)$$

This hierarchical regression analysis allowed us to test whether each block of factors explains unique variance in image ratings, over and beyond what is explained by previous blocks of factors. Notably, because the second block of factors should be expected to show a strong relationship with image ratings (due to selection bias, Kriegeskorte *et al.*, 2009), any additional explanatory power over and beyond these factors represents compelling support for the notion that multiple brain regions work in concert with pVMPFC to compute common currency.

RESULTS

Ratings and choice behavior

Our behavioral analyses provided several manipulation checks. First, we examined whether participants' attractiveness ratings were consistent with an independent sample (Smith *et al.*, 2010). To do this, we compared the difference in the average normalized ratings between the two categories (medium–high and medium–low) defined by our independent sample. This analysis revealed that participants rated the high-value images significantly higher than the low-value images (high-value mean: 3.44; low-value mean: 2.10; range of differences: 0.39 to 2.31; paired $t_{(12)} = 10.47$, $P < 0.001$). Second, we examined whether response time measures were related to trial-to-trial ratings or exchange rate. We found that the average reaction time across all trials was unrelated to exchange rate [$r_{(14)} = 0.01$, n.s.]. Further, for each participant, the trial-to-trial ratings were, on average, uncorrelated with the trial-to-trial response times (mean $r = 0.04$, SD = 0.16; range: −0.22 to 0.29), indicating that response times were largely independent of valuation measures. Finally, we also examined the relationship between the average attractiveness ratings for high-value images and the exchange rate between faces and money. Although ratings data and choice data can be decoupled (Knoch *et al.*, 2006), we found a modest correlation where higher attractiveness ratings for high-value images predicted increased willingness to purchase faces [$r_{(14)} = 0.56$, $P < 0.05$]. Thus, our core analyses regarding the interactions between pVMPFC and functionally connected brain regions will employ both valuation measures.

Parametric effects of attractiveness

To identify brain regions whose activation tracked attractiveness ratings, we examined the main effect of the first-order (linear) term in our parametric model. This analysis revealed that activation in several key regions increased with attractiveness: the dorsal anterior cingulate cortex (dACC), aVMPFC and caudate (Figure 2; Table 1 shows a representative listing of activation coordinates). We note that aVMPFC (MNI: x,y,z = 0,46,−8) overlaps with our previous work (Smith *et al.*, 2010), consistent with its role in encoding outcome value (Clithero and Rangel, 2013).

As a control analysis, we identified regions whose activation tracked the salience of the social rewards. Several regions exhibited a significant nonlinear relationship (quadratic, fitting the second term of our parametric model) with attractiveness ratings, including the anterior insula and MPFC (Table 2 shows a representative listing of activation coordinates). Activation in these regions followed a U-shaped pattern, with least response to medium attractiveness faces and greatest response to high and low attractiveness faces. No regions exhibited a significant negative relationship with the linear or quadratic predictor at our statistical threshold.

Increased functional connectivity with pVMPFC predicts social valuation

We next tested our core prediction that pVMPFC interacts—in a manner related to subjective value computation—with regions modulated by social information in our task. To do this, we conducted a PPI analysis using the participant-specific pVMPFC activation and attractiveness ratings. Importantly, we also introduced each participant's exchange rate as a covariate in the group level model (average: 0.42; range: 0.1–0.8). Therefore, this analysis highlights regions whose functional coupling with pVMPFC is modulated both by an individual's attractiveness ratings and by their willingness to exchange money for faces. Using this approach, we found a network of regions—including TPJ, MPFC, PCC and middle temporal gyrus (MTG)—whose functional connectivity with pVMPFC increases with increasing social reward valuation (Figure 3).

Nevertheless, it could be the case that connectivity with pVMPFC does not depend on trial-to-trial attractiveness ratings. To test this alternative model, we performed a post hoc PPI analysis in which the psychological context of interest is simply the presentation of a face (i.e. the unmodulated face regressor). This alternative psychological context is orthogonal to our primary analysis (i.e. increasing attractiveness judgments) and represents an uncontrolled visual stimulus and thus it allows us to test the alternative model that the results from Figure 3 depend not on attractiveness ratings but on the presentation of faces themselves. Yet, within this alternative model we failed to observe a significant association between pVMPFC connectivity and willingness to exchange money for faces. Moreover, the unthresholded statistical map was independent of the unthresholded results in Figure 3 (spatial correlation: 0.04), thus providing compelling evidence that the observed connectivity results are task specific and dependent on increasing attractiveness judgments.

Given the importance of controlling for motion in functional connectivity analyses, especially those involving individual differences (Power *et al.*, 2012; Satterthwaite *et al.*, 2012), we also examined whether the proportion of exchanges was correlated with individual differences in head motion. We did not observe a significant relationship between participant exchange rate and participant head motion, summarized as the coefficient of variation for absolute head motion across time [$r_{(14)} = -0.22$, n.s.].

Our primary functional connectivity analysis, while consistent with previous works (Hare *et al.*, 2010; Janowski *et al.*, 2013; van den Bos *et al.*, 2013), does not in itself test a key prediction regarding the relationship between value signals within pVMPFC and functionally connected regions: that activation of additional regions explains unique variability in the subjective value of social stimuli. We tested this prediction using hierarchical regression on the trial-to-trial attractiveness ratings with four distinct blocks of factors. Our first

Table 1 Regions tracking increasing value

Probabilistic anatomical label	x	y	z	*Z*-stat	Cluster volume (*P*)
Occipital pole (62%)	−4	−100	4	3.51	13 000 mm^3 ($P < 0.001$)
Occipital pole (25%), iLOC (6%), OFG (5%)	24	−90	0	3.25	
Occipital pole (35%)	−2	−100	−6	3.17	
Cuneal cortex (25%), sLOC (5%)	−14	−82	28	3.17	
Occipital pole (65%)	16	−96	−2	3.1	
ACC (61%), Paracingulate gyrus (25%)	6	18	34	3.8	12680 mm^3 ($P < 0.001$)
Juxtapositional lobule cortex (33%), SFG (12%)	0	8	60	3.43	
SFG (37%), Juxtapositional lobule cortex (20%)	6	10	70	3.36	
Juxtapositional lobule cortex (72%), ACC (5%)	−2	0	52	3.18	
ACC (64%), Juxtapositional lobule cortex (21%)	−2	4	42	3.15	
WM (98%)	28	−16	30	3.26	5832 mm^3 ($P < 0.01$)
WM (96%)	22	−16	24	3.22	
WM (99%)	20	−20	32	2.96	
Right lateral ventricle (81%)	2	2	16	2.95	
Left lateral ventricle (51%), right lateral ventricle (27%)	0	10	10	2.94	
Lingual gyrus (43%)	14	−68	−2	3.17	3808 mm^3 ($P < 0.05$)
Lingual gyrus (55%)	14	−56	−2	2.97	
OFG (47%), Lingual gyrus (12%), TOFC (10%)	28	−64	−10	2.94	
OFG (29%), iLOC (5%)	36	−66	−10	2.89	
Intracalcarine cortex (39%), Lingual gyrus (14%)	14	−64	4	2.88	
iLOC (33%), Occipital pole (5%)	−28	−88	0	3.19	3456 mm^3 ($P < 0.05$)
iLOC (9%)	−28	−82	2	3.17	
Occipital pole (67%)	−12	−100	18	2.84	
Occipital pole (51%)	−24	−96	4	2.82	
Occipital pole (19%), sLOC (16%)	−18	−90	16	2.76	

Regions whose activation increases with increasing social reward (Figure 2). Coordinates of the top five local maxima within each cluster of activation are in MNI space. We note that, due to cluster-based inference, individual voxels and peaks cannot be considered significant in themselves, as the inference is on the size of the cluster. Accordingly, we also note that the second largest cluster with a peak in ACC also contained aVMPFC [data not shown in table; (MNI: x,y,z = 0,46,−8)]. Probabilistic labels reflect the probability (or likelihood) that a coordinate belongs to a given region. For clarity, we only show labels whose likelihood exceeds 5%.
WM, white matter; sLOC, lateral occipital cortex, superior division; iLOC, lateral occipital cortex, inferior division; ACC, anterior cingulate cortex; OFG, occipital fusiform gyrus; SFG, superior frontal gyrus; TOFC, temporal occipital fusiform cortex.

Table 2 Regions tracking increasing salience

Probabilistic anatomical label	x	y	z	*Z*-stat	Cluster volume (*P*-value)
OFC (28%), Insula (12%)	26	14	−14	3.49	7040 mm^3 ($P < 0.001$)
Insula (68%)	38	14	−12	3.3	
Insula (34%)	32	14	−8	3.3	
OFC (43%), F operculum (13%), IFG (10%)	42	28	−6	3.1	
OFC (32%), IFG (27%), F operculum (12%)	50	28	−6	2.96	
ParaCG (48%), ACC (13%), MPFC (7%)	−10	46	−2	3.29	6832 mm^3 ($P < 0.001$)
ACC (15%), ParaCG (6%)	−10	36	−2	3.1	
ParaCG (72%), ACC (10%)	10	48	8	3.09	
ParaCG (44%), ACC (24%)	10	44	0	3.05	
ACC (25%)	0	22	16	2.99	

Regions whose activation follows a nonlinear, U-shaped pattern in response to social reward. Coordinates of the top five local maxima within each cluster of activation are in MNI space. We note that, due to cluster-based inference, individual voxels and peaks cannot be considered significant in themselves, as the inference is on the size of the cluster. Probabilistic labels reflect the probability (or likelihood) that a coordinate belongs to a given region. For clarity, we only show labels whose likelihood exceeds 5%.
OFC, frontal orbital cortex; IFG, inferior frontal gyrus, pars triangularis; MPFC, frontal medial cortex; ParaCG, paracingulate gyrus; F Operculum, frontal operculum cortex; ACC, anterior cingulate cortex

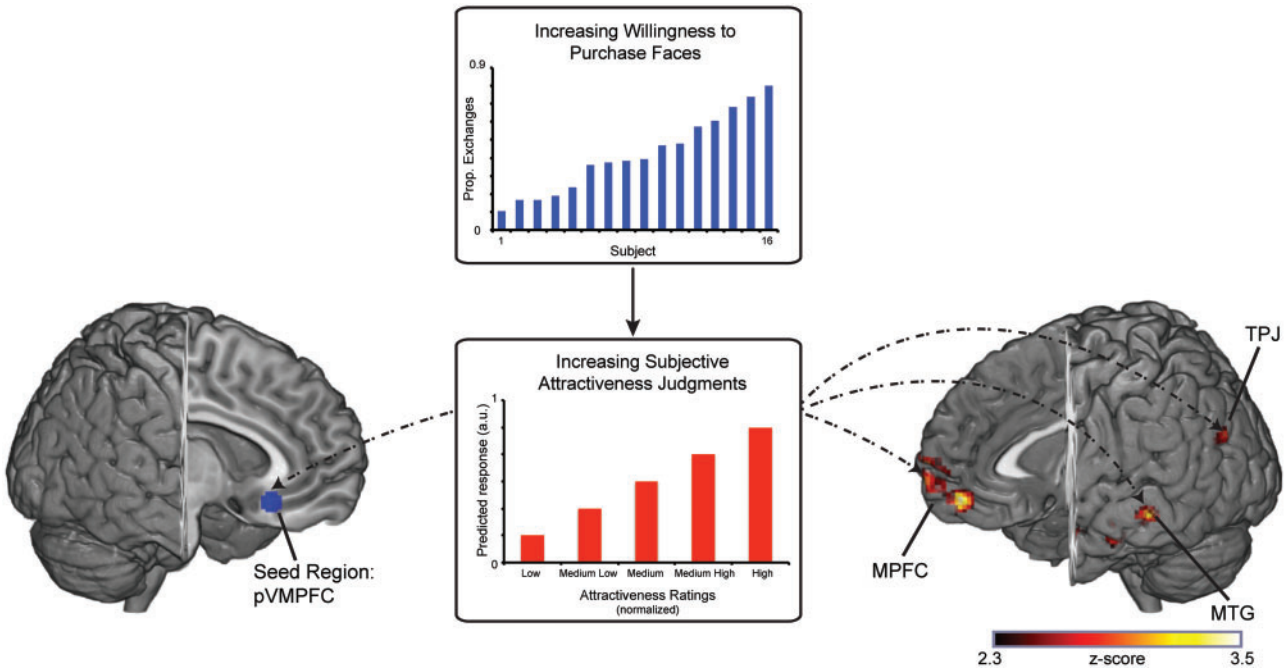

Fig. 3 Functional connectivity with posterior VMPFC predicts social valuations. We employed a PPI analysis to identify regions whose functional connectivity with pVMPFC increases as a function of both increasing attractiveness ratings and increasing willingness to exchange money for faces. Shown on the left is a depiction of our seed region, pVMPFC (x,y,z = 6,26,−14), which was chosen based on our previous work (Smith *et al.*, 2010). The middle panel shows a schematic of the trial-to-trial modulator (subjective attractiveness) and the participant covariate (proportion of exchanges). Shown on the right are areas whose connectivity with pVMPFC increases with increasing attractiveness ratings and increasing willingness to trade money for faces. These regions included the MPFC (x,y,z = 4,70,−4), TPJ (x,y,z = −40,−60,32), middle temporal gyrus (MTG) (x,y,z = −66,−32,−6) and PCC (x,y,z = −2,−46,20). All areas of activation passed an initial cluster-forming threshold of $z = 2.3$, with whole-brain cluster correction at $P = 0.05$ (corrected for multiple comparisons).

block of factors [Block 1; see equation (1)] controlled for nuisance predictors, including response time, session number, trial number and participant identity. Next, we added a second block of factors [Block 2; see equation (2)] that included activation estimates from five regions responsive to attractiveness ratings (see cluster peaks within Table 1) and introduced the trial-by-trial parameter estimates from aVMPFC and pVMPFC (Smith *et al.*, 2010). As expected, these factors significantly improved the fit of our model, explaining unique variance over and beyond what is explained by Block 1 alone (Table 4). We then added a third block of factors [Block 3; see equation (3)] that introduced the trial-by-trial activation estimates from each of the four regions whose functional connectivity with pVMPFC increased with increasing social valuation (Table 3). Strikingly, we found that signals from these additional regions explained additional variance in subjective valuations over and above what was observed by Blocks 1 and 2 together (Table 4). The final level of our model introduced the interaction terms between pVMPFC and each of the four PPI regions (see Equation 4); however, these additional factors failed to explain additional variance over and above what was explained by previous blocks of factors. Complete regression statistics corresponding to individual factors are provided in Table 5.

DISCUSSION

Decision neuroscience has made considerable progress toward identifying signals in pVMPFC that encode disparate rewards on a common scale (for review, Levy and Glimcher, 2012). This observation has sparked new lines of inquiry regarding how relevant information modulates value computation in pVMPFC. Here, we show that pVMPFC increases connectivity with a network of regions modulated by social information in our task, and that these increases in connectivity depend on individual differences in subjective valuations for social reward. Our results also indicate that the network of regions exhibiting functional connectivity with pVMPFC—the TPJ, MTG, PCC and MPFC—explain unique variation in a hierarchical regression modeling trial-to-trial fluctuations in social valuation. These findings endorse the idea that interacting brain systems contribute to the computation of the subjective value for social rewards, a result consistent with studies of common currency processing in VMPFC (Levy and Glimcher, 2012).

Our findings are consistent with an emerging body of research suggesting that pVMPFC interacts with other brain systems during valuation, potentially in a context-specific manner (Clithero and Rangel, 2013). For example, dietary decisions involving self control evoke activation in dorsolateral prefrontal cortex (DLPFC), which exhibits increased functional connectivity with VMPFC (Hare *et al.*, 2009). In addition, other work has indicated that connectivity between pVMPFC and regions within the inferior parietal lobe increases during empathy (Janowski *et al.*, 2013), charitable donations (Hare *et al.*, 2010) and social competition (van den Bos *et al.*, 2013). Yet, observing functional connectivity between pVMPFC and other regions does not in itself demonstrate that interacting brain regions construct subjective value signals. Our study therefore extends prior observations by showing that individual differences in subjective value for social stimuli modulate the strength of connectivity between pVMPFC and regions modulated by social information. Crucially, we also show that activation estimates from these additional regions explain unique variation in social valuations. However, like other studies utilizing PPI, we note that our results cannot speak to the directionality of information flow. Future studies could therefore utilize other methods, to gain insight into the directionality of interactions between pVMPFC and the network of regions modulated by social information.

Unlike previous studies highlighting interactions between this network of regions and pVMPFC (Hare *et al.*, 2010; Janowski *et al.*, 2013), our paradigm required actively evaluating other people's faces.

Table 3 Regions exhibiting connectivity with posterior VMPFC

Probabilistic anatomical label	x	y	z	*Z*-stat	Cluster volume (*P*-value)
pMTG (75%), pSTG (9%)	−66	−32	−6	3.35	4168 mm^3 ($P < 0.05$)
pSTG (63%), pMTG (12%)	−64	−28	2	3.26	
pMTG (22%), MTG temporooccipital part (16%)	−56	−42	−6	3.17	
pMTG (9%)	−72	−34	−4	3.09	
pMTG (26%), aMTG (24%),	−56	−10	−20	3	
sLOC (21%), Angular Gyrus (8%), iLOC (7%)	−38	−62	18	3.37	4128 mm^3 ($P < 0.05$)
sLOC (23%), Angular Gyrus (21%)	−42	−60	36	3.14	
Angular Gyrus (23%), sLOC (15%)	−40	−60	32	3.07	
sLOC (34%)	−36	−68	34	2.95	
Angular Gyrus (18%)	−36	−60	26	2.95	
PCC (8%), Posterior Parahippocampal Gyrus (5%)	−6	−42	0	3.36	3704 mm^3 ($P < 0.05$)
Precuneus Cortex (30%)	−16	−54	10	3.27	
PCC (56%), Precuneus Cortex (13%)	−10	−48	4	3.03	
PCC (81%)	−2	−46	20	2.92	
PCC (19%), Precuneus Cortex (6%)	8	−46	18	2.91	
Frontal Medial Cortex (71%), Frontal Pole (13%)	2	52	−12	3.5	3464 mm^3 ($P < 0.05$)
Frontal Pole (67%)	4	70	4	3.25	
Frontal Pole (57%)	4	70	−4	3.08	
Frontal Pole (45%)	−2	68	4	3.03	
Frontal Pole (47%)	0	66	−8	2.99	

Regions whose functional connectivity with posterior VMPFC increases as a function of increasing attractiveness ratings and increasing economic exchanges (Figure 3). Coordinates of the top five local maxima within each cluster of activation are in MNI space. We note that, due to cluster-based inference, individual voxels and peaks cannot be considered significant in themselves, as the inference is on the size of the cluster. Probabilistic labels reflect the probability (or likelihood) that a coordinate belongs to a given region. For clarity, we only show labels whose likelihood exceeds 5%.
pMTG, middle temporal gyrus, posterior division; pSTG, superior temporal gyrus, posterior division; aMTG, middle temporal gyrus, anterior division; sLOC, lateral occipital cortex, superior division; iLOC, lateral occipital cortex, inferior division; ACC, anterior cingulate cortex; PCC, posterior cingulate cortex.

Table 4 Hierarchical regression results

Block	*F*-stat	Block DF	Block Residual	R^2	Change in R^2	*P*-value
1	4.15	18	692	0.0884		0
2	2.05	14	678	0.1265	0.0383	0.0125
3	3.56	8	670	0.1614	0.0349	0.0005
4	1.17	8	662	0.1730	0.0116	0.3164

To examine the incremental contribution of additional regions of interest, we performed a hierarchical regression analysis with four sequential levels: confound terms [Block 1; see equation (1)]; value terms [Block 2; see equation (2)]; functional connectivity terms [Block 3; see equation (3)]; interaction terms [Block 4; see equation (4)]. Our analysis indicated that activation estimates derived from regions functionally connected to posterior VMPFC explained unique variance in trial-to-trial image ratings, over and beyond what was observed from activation estimates in regions modulated by value alone.

Table 5 Complete regression statistics

Block number	Factor	β	VIF	Robust SE	*t*-stat	*P*-value
1	Response time	0.0779	1.49	0.061	1.27	0.204
1	Trial number	−0.0042	1.10	0.002	−1.73	0.083
1	Run number	0.0305	1.31	0.055	0.56	0.577
2	aVMPFC	0.0887	2.63	0.053	1.67	0.096
2	pVMPFC	0.0230	1.62	0.038	0.60	0.548
2	linear_ACC	0.1105	1.28	0.036	3.03	0.003
2	linear_VC1	0.0600	1.34	0.034	1.74	0.082
2	linear_VC2	0.0228	1.53	0.038	0.60	0.549
2	linear_VC3	0.0693	1.35	0.034	2.03	0.043
2	linear_WM	0.0203	1.19	0.033	0.61	0.540
2	exchanges*aVMPFC	−0.1519	2.51	0.083	−1.83	0.068
2	exchanges*pVMPFC	0.0874	1.67	0.066	1.33	0.185
2	exchanges*linear_ACC	−0.0267	1.32	0.065	−0.41	0.679
2	exchanges*linear_VC1	0.0578	1.39	0.062	0.94	0.349
2	exchanges*linear_VC2	−0.0073	1.75	0.070	−0.10	0.917
2	exchanges*linear_VC3	−0.0533	1.33	0.057	−0.93	0.351
2	exchanges*linear_WM	0.0628	1.21	0.056	1.13	0.260
3	ppi_RSP	0.0444	1.47	0.038	1.17	0.243
3	ppi_TPJ	−0.0713	1.35	0.035	−2.06	0.040
3	ppi_MPFC	−0.0788	2.14	0.051	−1.55	0.121
3	ppi_MTG	−0.1122	1.36	0.035	−3.23	0.001
3	exchanges*ppi_RSP	−0.0018	1.59	0.072	−0.03	0.979
3	exchanges*ppi_TPJ	−0.1001	1.45	0.064	−1.56	0.120
3	exchanges*ppi_MPFC	0.0219	2.04	0.081	0.27	0.786
3	exchanges*ppi_MTG	0.0490	1.35	0.065	0.76	0.450
4	ppi_RSP*pVMPFC	−0.0146	1.48	0.044	−0.33	0.743
4	ppi_TPJ*pVMPFC	−0.0373	1.41	0.041	−0.90	0.367
4	ppi_MPFC*pVMPFC	0.0376	1.44	0.050	0.75	0.454
4	ppi_MTG*pVMPFC	0.0090	1.41	0.045	0.20	0.840
4	exchanges*ppi_RSP*pVMPFC	−0.0501	1.72	0.083	−0.60	0.547
4	exchanges*ppi_TPJ*pVMPFC	0.0662	1.58	0.075	0.88	0.380
4	exchanges*ppi_MPFC*pVMPFC	0.0887	1.64	0.082	1.09	0.278
4	exchanges*ppi_MTG*pVMPFC	0.1237	1.48	0.078	1.59	0.112

The full regression model included four blocks, each with several regressors. For clarity, we omit dummy regressors in the table for participants, which were included in Block 1. Aside from pVMPFC and aVMPFC (which overlapped with the large ACC cluster in Table 1), all regions are cluster peaks derived from our analyses. We also summarize the severity of multicollinearity for each regressor using variance inflation factor (VIF). As all VIF values are <5 and similar across blocks, we can be confident that multicollinearity did not bias our results (Kutner *et al.*, 2004).

Viewing images of faces triggers evaluations of the social category, identity, emotion and psychological disposition of each face (Zebrowitz, 2006); these evaluative processes may evoke self-referential thoughts, thus modulating activation in midline regions such as the MPFC and PCC (Whitfield-Gabrieli *et al.*, 2011). Facial attractiveness also conveys reproductive fitness information (Little *et al.*, 2008). Beyond fitness information, faces are important features in dynamic social interactions requiring assessment of intentions and motives (e.g. cooperation) (Mende-Siedlecki *et al.*, 2013)—processes that are likely modulated by additional factors, such as social closeness (Fareri *et al.*, 2012). Notably, other studies examining face perception have implicated the amygdala (Mende-Siedlecki *et al.*, 2013), which was not observed in our study, possibly due to a limited dynamic range of attractiveness (Winston *et al.*, 2007) or naturalistic qualities of face stimuli (Mende-Siedlecki *et al.*, 2013). Taken together, our results are broadly consistent with other studies requiring active evaluation of facial stimuli.

Yet, we note that the use of faces within the constraints of our paradigm give rise to interpretive challenges that are worth additional consideration. For example, attractive faces—like all rewards with social properties—may not be purely social in nature and hence our results could, in part, reflect evaluative processes that are not specific to social stimuli. Future studies could control for this issue by contrasting attractiveness judgments for attractive faces to attractiveness judgments for non-social visual images (e.g. attractive scenes). Indeed, this analysis could also provide greater insight into the computation of a common currency, as idiosyncratic differences in neural responses to social and non-social reward could be matched to behavioral preferences between social and non-social rewards (Smith *et al.*, 2010). Strictly speaking, our results are thus limited to subjective value (i.e. the relative decision value between attractive faces and money), which is a necessary but not sufficient condition for identifying neural signals related to the construction of common currency (Levy and Glimcher, 2012).

Another consideration is how the subjective ratings during the evaluation period in our fMRI task map onto choices after scanning. Although we did find a modest correlation between subjective ratings and willingness to purchase faces, other studies have found discrepancies between different measures of value, depending upon the

elicitation method (Grether and Plott, 1979; Knoch *et al.*, 2006). Nevertheless, we emphasize that previous studies examining value computations have found consistent results using passive viewing of items presented individually (Smith *et al.*, 2010) and active choices between two items presented simultaneously (Levy and Glimcher, 2011).

Our discussion has focused on the social component of functional networks contributing to subjective value, but there are alternative explanations involving non-social computations and functional connectivity with VMPFC. For example, one prominent theory argues that TPJ supports bottom–up attention (Cabeza *et al.*, 2012). Although we controlled for response time differences across valuations and activation profiles tracking salience, we note that attentional factors might influence our results. Indeed, recent work suggests that value signals in VMPFC are guided by attention (Lim *et al.*, 2011), possibly originating from salience computations within TPJ (Kahnt and Tobler, 2013). In contrast, other findings have pointed to a specialized role for TPJ in social perception (Gao *et al.*, 2012) and social decision making (Carter *et al.*, 2012). Given these divergent findings, we speculate that the TPJ carries out multiple functions for decision making—both social and attentional—depending on its connectivity patterns with other brain regions (Mars *et al.*, 2012; Nelson *et al.*, 2012; Carter and Huettel, 2013).

We conclude that our data are consistent with the idea that a distributed network of brain regions contributes value-related information that interacts with signals in pVMPFC to establish subjective value. These computations appear to be idiosyncratic and are thus likely influenced by additional variables affecting motivation (Strauman *et al.*, 2013), emotion (Winecoff *et al.*, 2013) and social closeness (Fareri *et al.*, 2012). More broadly, our study also suggests that models of brain networks—as opposed to single regions—may help understand variability in decision processes across people (Levallois *et al.*, 2012). Indeed, the idea of focusing on brain networks is already advancing insights into clinical syndromes (Smith *et al.*, 2013) and neurogenetics (Tost *et al.*, 2012). We speculate that applying similar principles to social valuation may lead to improved models of pathological social decision making, as observed in autism (Izuma *et al.*, 2011) and anorexia nervosa (Watson *et al.*, 2010).

REFERENCES

Baumgartner, T., Knoch, D., Hotz, P., Eisenegger, C., Fehr, E. (2011). Dorsolateral and ventromedial prefrontal cortex orchestrate normative choice. *Nature Neuroscience*, *14*(11), 1468–74.

Beckmann, C.F., Jenkinson, M., Smith, S.M. (2003). General multilevel linear modeling for group analysis in FMRI. *Neuroimage*, *20*(2), 1052–63.

Behrens, T.E., Hunt, L.T., Rushworth, M.F. (2009). The computation of social behavior. *Science*, *324*(5931), 1160–4.

Brainard, D.H. (1997). The psychophysics toolbox. *Spatial Vision*, *10*, 443–6.

Buchel, C., Holmes, A.P., Rees, G., Friston, K.J. (1998). Characterizing stimulus-response functions using nonlinear regressors in parametric FMRI experiments. *Neuroimage*, *8*(2), 140–8.

Cabeza, R., Ciaramelli, E., Moscovitch, M. (2012). Cognitive contributions of the ventral parietal cortex: an integrative theoretical account. *Trends in Cognitive Science*, *16*(6), 338–52.

Carter, R.M., Bowling, D.L., Reeck, C., Huettel, S.A. (2012). A distinct role of the temporal-parietal junction in predicting socially guided decisions. *Science*, *337*(6090), 109–11.

Carter, R.M., Huettel, S.A. (2013). A nexus model of the temporal-parietal junction. *Trends in Cognitive Science*, *17*(7), 328–336.

Chib, V.S., Rangel, A., Shimojo, S., O'Doherty, J.P. (2009). Evidence for a common representation of decision values for dissimilar goods in human ventromedial prefrontal cortex. *Journal of Neuroscience*, *29*(39), 12315–20.

Clithero, J.A., Rangel, A. (2013). Informatic parcellation of the network involved in the computation of subjective value. *Social Cognitive and Affective Neuroscience*, *9*(9), 1289–1302.

Clithero, J.A., Reeck, C., Carter, R.M., Smith, D.V., Huettel, S.A. (2011a). Nucleus accumbens mediates relative motivation for rewards in the absence of choice. *Frontiers in Human Neuroscience*, *5*, 87.

Clithero, J.A., Smith, D.V., Carter, R.M., Huettel, S.A. (2011b). Within- and cross-participant classifiers reveal different neural coding of information. *Neuroimage*, *56*(2), 699–708.

Desikan, R.S., Segonne, F., Fischl, B., et al. (2006). An automated labeling system for subdividing the human cerebral cortex on MRI scans into gyral based regions of interest. *Neuroimage*, *31*(3), 968–80.

Fareri, D.S., Niznikiewicz, M.A., Lee, V.K., Delgado, M.R. (2012). Social network modulation of reward-related signals. *Journal of Neuroscience*, *32*(26), 9045–52.

Fehr, E., Camerer, C.F. (2007). Social neuroeconornics: the neural circuitry of social preferences. *Trends in Cognitive Science*, *11*(10), 419–27.

FitzGerald, T.H., Seymour, B., Dolan, R.J. (2009). The role of human orbitofrontal cortex in value comparison for incommensurable objects. *Journal of Neuroscience*, *29*(26), 8388–95.

Friston, K.J., Buechel, C., Fink, G.R., et al. (1997). Psychophysiological and modulatory interactions in neuroimaging. *Neuroimage*, *6*(3), 218–29.

Gao, T., Scholl, B.J., McCarthy, G. (2012). Dissociating the detection of intentionality from animacy in the right posterior superior temporal sulcus. *Journal of Neuroscience*, *32*(41), 14276–80.

Grether, D.M., Plott, C.R. (1979). Economic theory of choice and the preference reversal phenomenon. *The American Economic Review*, *69*(4), 623–38.

Hare, T.A., Camerer, C.F., Knoepfle, D.T., Rangel, A. (2010). Value computations in ventral medial prefrontal cortex during charitable decision making incorporate input from regions involved in social cognition. *Journal of Neuroscience*, *30*(2), 583–90.

Hare, T.A., Camerer, C.F., Rangel, A. (2009). Self-control in decision-making involves modulation of the VMPFC valuation system. *Science*, *324*(5927), 646–8.

Hasson, U., Ghazanfar, A.A., Galantucci, B., Garrod, S., Keysers, C. (2012). Brain-to-brain coupling: a mechanism for creating and sharing a social world. *Trends in Cognitive Science*, *16*(2), 114–21.

Izuma, K., Matsumoto, K., Camerer, C.F., Adolphs, R. (2011). Insensitivity to social reputation in autism. *Proceedings of the National Academy of Sciences, USA*, *108*(42), 17302–7.

Izuma, K., Saito, D.N., Sadato, N. (2008). Processing of social and monetary rewards in the human striatum. *Neuron*, *58*(2), 284–94.

Janowski, V., Camerer, C., Rangel, A. (2013). Empathic choice involves VMPFC value signals that are modulated by social processing implemented in IPL. *Social Cognitive and Affective Neuroscience*, *8*(2), 201–8.

Jenkinson, M., Bannister, P., Brady, M., Smith, S. (2002). Improved optimization for the robust and accurate linear registration and motion correction of brain images. *Neuroimage*, *17*(2), 825–41.

Jenkinson, M., Smith, S. (2001). A global optimisation method for robust affine registration of brain images. *Medical Image Analysis*, *5*(2), 143–56.

Kahnt, T., Tobler, P.N. (2013). Salience signals in the right temporoparietal junction facilitate value-based decisions. *Journal of Neuroscience*, *33*(3), 863–9.

Kim, H., Shimojo, S., O'Doherty, J.P. (2011). Overlapping responses for the expectation of juice and money rewards in human ventromedial prefrontal cortex. *Cerebral Cortex*, *21*(4), 769–76.

Knoch, D., Pascual-Leone, A., Meyer, K., Treyer, V., Fehr, E. (2006). Diminishing reciprocal fairness by disrupting the right prefrontal cortex. *Science*, *314*(5800), 829–32.

Kriegeskorte, N., Simmons, W.K., Bellgowan, P.S., Baker, C.I. (2009). Circular analysis in systems neuroscience: the dangers of double dipping. *Nature Neuroscience*, *12*(5), 535–40.

Kutner, M., Nachtsheim, C., Neter, J. (2004). *Applied Linear Regression Models* 4th edn. New York, NY: McGraw-Hill/Irwin.

Levallois, C., Clithero, J.A., Wouters, P., Smidts, A., Huettel, S.A. (2012). Translating upwards: linking the neural and social sciences via neuroeconomics. *Nature Reviews: Neuroscience*, *13*(11), 789–97.

Levy, D.J., Glimcher, P.W. (2011). Comparing apples and oranges: using reward-specific and reward-general subjective value representation in the brain. *Journal of Neuroscience*, *31*(41), 14693–707.

Levy, D.J., Glimcher, P.W. (2012). The root of all value: a neural common currency for choice. *Current Opinion in Neurobiology*, *22*(6), 1027–38.

Libedinsky, C., Smith, D.V., Teng, C.S., et al. (2011). Sleep deprivation alters valuation signals in the ventromedial prefrontal cortex. *Frontiers in Behavioral Neuroscience*, *5*, 70.

Lim, S.L., O'Doherty, J.P., Rangel, A. (2011). The decision value computations in the VMPFC and striatum use a relative value code that is guided by visual attention. *Journal of Neuroscience*, *31*(37), 13214–23.

Lin, A., Adolphs, R., Rangel, A. (2012). Social and monetary reward learning engage overlapping neural substrates. *Social Cognitive and Affective Neuroscience*, *7*(3), 274–81.

Little, A.C., Jones, B.C., Waitt, C., et al. (2008). Symmetry Is related to sexual dimorphism in faces: data across culture and species. *PLoS One*, *3*(5), e2106.

Mars, R.B., Sallet, J., Schüffelgen, U., et al. (2012). Connectivity-based subdivisions of the human right "temporoparietal junction area": Evidence for different areas participating in different cortical networks. *Cerebral Cortex*, *22*(8), 1894–903.

Mende-Siedlecki, P., Said, C.P., Todorov, A. (2013). The social evaluation of faces: a meta-analysis of functional neuroimaging studies. *Social Cognitive and Affective Neuroscience*, *8*(3), 285–99.

Nelson, S.M., McDermott, K.B., Petersen, S.E. (2012). In favor of a 'fractionation' view of ventral parietal cortex: comment on Cabeza et al. *Trends in Cognitive Science*, *16*(8), 399–400, author reply 400–391.

O'Doherty, J.P., Winston, J., Critchley, H., et al. (2003). Beauty in a smile: the role of medial orbitofrontal cortex in facial attractiveness. *Neuropsychologia*, *41*(2), 147–55.
O'Reilly, J.X., Woolrich, M.W., Behrens, T.E., Smith, S.M., Johansen-Berg, H. (2012). Tools of the trade: psychophysiological interactions and functional connectivity. *Social Cognitive and Affective Neuroscience*, *7*(5), 604–9.
Padoa-Schioppa, C. (2011). Neurobiology of economic choice: a good-based model. *Annual Review of Neuroscience*, *34*(1), 333–59.
Park, S.Q., Kahnt, T., Rieskamp, J., Heekeren, H.R. (2011). Neurobiology of value integration: when value impacts valuation. *Journal of Neuroscience*, *31*(25), 9307–14.
Power, J.D., Barnes, K.A., Snyder, A.Z., Schlaggar, B.L., Petersen, S.E. (2012). Spurious but systematic correlations in functional connectivity MRI networks arise from subject motion. *Neuroimage*, *59*(3), 2142–54.
Rangel, A., Hare, T. (2010). Neural computations associated with goal-directed choice. *Current Opinion in Neurobiology*, *20*(2), 262–70.
Rissman, J., Gazzaley, A., D'Esposito, M. (2004). Measuring functional connectivity during distinct stages of a cognitive task. *Neuroimage*, *23*(2), 752–63.
Rorden, C., Karnath, H.O., Bonilha, L. (2007). Improving lesion-symptom mapping. *Journal of Cognitive Neuroscience*, *19*(7), 1081–8.
Roy, M., Shohamy, D., Wager, T.D. (2012). Ventromedial prefrontal-subcortical systems and the generation of affective meaning. *Trends in Cognitive Science*, *16*(3), 147–56.
Rushworth, M.F., Noonan, M.P., Boorman, E.D., Walton, M.E., Behrens, T.E. (2011). Frontal cortex and reward-guided learning and decision-making. *Neuron*, *70*(6), 1054–69.
Satterthwaite, T.D., Wolf, D.H., Loughead, J., et al. (2012). Impact of in-scanner head motion on multiple measures of functional connectivity: relevance for studies of neurodevelopment in youth. *Neuroimage*, *60*(1), 623–32.
Saxe, R. (2006). Uniquely human social cognition. *Current Opinion in Neurobiology*, *16*(2), 235–9.
Smith, D.V., Clithero, J.A., Rorden, C., Karnath, H.O. (2013). Decoding the anatomical network of spatial attention. *Proceedings of the National Academy of Sciences, USA*, *110*(4), 1518–23.
Smith, D.V., Hayden, B.Y., Truong, T.K., et al. (2010). Distinct value signals in anterior and posterior ventromedial prefrontal cortex. *Journal of Neuroscience*, *30*(7), 2490–5.
Smith, D.V., Huettel, S.A. (2010). Decision neuroscience: neuroeconomics. *Wiley Interdisciplinary Reviews Cognitive Science*, *1*(6), 854–71.
Smith, S.M. (2002). Fast robust automated brain extraction. *Human Brain Mapping*, *17*(3), 143–55.
Smith, S.M., Jenkinson, M., Woolrich, M.W., et al. (2004). Advances in functional and structural MR image analysis and implementation as FSL. *Neuroimage*, *23*(Suppl 1), S208–19.
Strauman, T.J., Detloff, A.M., Sestokas, R., et al. (2013). What shall I be, what must I be: neural correlates of personal goal activation. *Frontiers in Integrative Neuroscience*, *6*, 123.
Tost, H., Bilek, E., Meyer-Lindenberg, A. (2012). Brain connectivity in psychiatric imaging genetics. *Neuroimage*, *62*(4), 2250–60.
van den Bos, W., Talwar, A., McClure, S.M. (2013). Neural correlates of reinforcement learning and social preferences in competitive bidding. *Journal of Neuroscience*, *33*(5), 2137–46.
Vickery Timothy, J., Chun Marvin, M., Lee, D. (2011). Ubiquity and specificity of reinforcement signals throughout the human brain. *Neuron*, *72*(1), 166–77.
Wallis, J.D. (2012). Cross-species studies of orbitofrontal cortex and value-based decision-making. *Nature Neuroscience*, *15*(1), 13–19.
Watson, K.K., Werling, D.M., Zucker, N.L., Platt, M.L. (2010). Altered social reward and attention in anorexia nervosa. *Frontiers in Psychology*, *1*, 36.
Whitfield-Gabrieli, S., Moran, J.M., Nieto-CastaÒÛn, A., et al. (2011). Associations and dissociations between default and self-reference networks in the human brain. *Neuroimage*, *55*(1), 225–32.
Winecoff, A., Clithero, J.A., Carter, R.M., et al. (2013). Ventromedial prefrontal cortex encodes emotional value. *The Journal of Neuroscience*, *33*(27), 11032–9.
Winston, J.S., O'Doherty, J., Kilner, J.M., Perrett, D.I., Dolan, R.J. (2007). Brain systems for assessing facial attractiveness. *Neuropsychologia*, *45*(1), 195–206.
Woolrich, M. (2008). Robust group analysis using outlier inference. *Neuroimage*, *41*(2), 286–301.
Woolrich, M.W., Behrens, T.E., Beckmann, C.F., Jenkinson, M., Smith, S.M. (2004). Multilevel linear modelling for FMRI group analysis using Bayesian Inference. *Neuroimage*, *21*(4), 1732–47.
Woolrich, M.W., Jbabdi, S., Patenaude, B., et al. (2009). Bayesian analysis of neuroimaging data in FSL. *Neuroimage*, *45*(Suppl. 1), S173–86.
Woolrich, M.W., Ripley, B.D., Brady, M., Smith, S.M. (2001). Temporal autocorrelation in univariate linear modeling of FMRI data. *Neuroimage*, *14*(6), 1370–86.
Worsley, K.J. (2001). Statistical analysis of activation images. In: Jezzard, P., Matthews, P.M., Smith, S.M., editors. *Functional MRI: An Introduction to Methods*. USA: Oxford University Press.
Zaki, J., López, G., Mitchell, J.P. (2013). Activity in ventromedial prefrontal cortex covaries with revealed social preferences: evidence for person-invariant value. *Social Cognitive and Affective Neuroscience*, *9*(4), 464–69.
Zebrowitz, L.A. (2006). Finally, faces find favor. *Social Cognition*, *24*(5), 657–701.
Zilles, K., Amunts, K. (2010). Centenary of Brodmann's map–conception and fate. *Nature Reviews: Neuroscience*, *11*(2), 139–45.